

Spontaneously bended nematic and antiferroelectric smectic structures of banana-shaped hard particles in two dimensions

This article has been downloaded from IOPscience. Please scroll down to see the full text article.

2012 EPL 97 26004

(<http://iopscience.iop.org/0295-5075/97/2/26004>)

View [the table of contents for this issue](#), or go to the [journal homepage](#) for more

Download details:

IP Address: 149.156.89.220

The article was downloaded on 24/05/2012 at 19:18

Please note that [terms and conditions apply](#).

Spontaneously bended nematic and antiferroelectric smectic structures of banana-shaped hard particles in two dimensions

J. A. MARTÍNEZ-GONZÁLEZ¹, S. VARGA², P. GURIN² and J. QUINTANA-H.^{2(a)}

¹ *Instituto de Química, Universidad Nacional Autónoma de México - Apdo. Postal 70213, 04510 Coyoacán, México D.F., México*

² *Institute of Physics and Mechatronics, University of Pannonia - PO Box 158, Veszprém, H-8201 Hungary, EU*

received 1 September 2011; accepted in final form 6 December 2011

published online 17 January 2012

PACS 64.70.mf – Theory and modeling of specific liquid crystal transitions, including computer simulation

PACS 61.30.Cz – Molecular and microscopic models and theories of liquid crystal structure

PACS 05.20.Jj – Statistical mechanics of classical fluids

Abstract – Spontaneously deformed nematic and antiferroelectric smectic structures have been detected in a two-dimensional system of hard banana-shaped needles by means of Monte Carlo simulation and Onsager theory. The spatially non-uniform and deformed nematic consists of orientationally ordered polar domains, where the nematic director displays mainly bended patterns. The net polarization of the bended nematic is zero. Onsager theory shows that the bent-core structure of the particles favours the bend deformation due to a free energy reducing bend torque, while the splay deformation results in a free energy cost. With increasing pressure the polar nematic domains becomes thinner and transforms into linear arrays with alternating polarity (antiferroelectric smectic phase). The theoretical results are in good agreement with the simulations.

Copyright © EPLA, 2012

Introduction. – Bent-core molecules, which are often referred to as bananas, have received considerable experimental and theoretical attention over the past years due to the discovery of the biaxial nematic phase [1–4] and tilted smectic phases with polar layers [5–7]. These phases are relevant in the technology as they can be used in fast electro-optical devices [8]. At first sight the formation of the biaxial nematic phase is understandable in the system of bent-core molecules due to the biaxial molecular symmetry. However it is very hard to stabilize the biaxial nematic order by purely steric forces due to the strong competition between the orientational and packing entropies. While the packing entropy gain is always significant for the alignment of the long molecular axes, the ordering of the short axes do not improve the packing of the rods notably and the more ordered smectic and columnar phases also come into the competition by resulting very complex phase diagrams [9]. The stabilization of ferroelectric smectic and columnar phases (B_n mesophases) in bent-core systems is even surprising because these phases were attributed to chiral units of the mesogens. It is astonishing that chiral domains can form

spontaneously even if the constituting molecules are achiiral [6]. Evidently the anisotropic steric interactions play important role in the formation of B_n phases, because the packing is more efficient with a tilt in the spatially ordered phases [10].

No doubt, the orientational and positional restriction affects dramatically the stability of the banana phases, too. For example, the extensively studied two-dimensional (2D) system of hard needles with zero thickness do exhibit isotropic and quasi-long-range nematic phases, while spatially ordered phases do not take place at all [11]. The latter result is due to the fact that there is no packing entropy gain from the positional ordering since the system of parallel hard needles behaves like an “ideal gas”. The orientational fluctuations are more significant in 2D than in 3D by reducing the true long-range nematic order into an algebraically decaying orientational order. As a result the first-order isotropic-nematic phase transition of three-dimensional systems transforms into a continuous Kosterlitz-Thouless-type isotropic-nematic transition [12]. The scenario seems to be more complicated in the case of 2D bananas because of the polar shape of the particles. The nematic order must be less favourable (or even missing) because the bent-core shape does not support so

^(a)E-mail: jaq@unam.mx

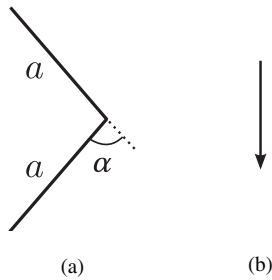


Fig. 1: a) Hard body representation of a banana-shaped molecule consisting of two equal line segments with length a and bend angle α between them. b) Definition of the polar axis of the molecule. The total length of the particle is $L = 2a$.

much the orientational order without the positional one. On the other hand, the polar shape of the particles raises the issue of the polar nematic order. Moreover, the smectic order cannot be ruled out as the particles can pack more efficiently in the layered structure. In this regard several experimental studies have been devoted to the effect of orientational and spatial restriction on the phase behaviour of the bent-core molecules [13–16]. Even strictly 2D system can be constructed by adsorbing banana-shaped P-n-PIMB molecules onto a HOPG surface. Gong and Wan [13] have observed several smectic-type orders like the antiferroelectric and bilayered smectic structures.

To the best of our knowledge, the simplest model of 2D bananas, which can be constructed from two identical straight lines joint at the ends by a given bend angle, see fig. 1, has not been studied by Monte Carlo simulation and Onsager theory. In this regard we are only aware of the recent study of Bisi *et al.* [17], where antiferroelectric smectic order is predicted in the 2D system of V-shaped particles on the basis of packing arguments.

Simulation. – In this work we study the global phase behaviour of the system of bent-core needles in two dimensions, where the particles are allowed to move and rotate in the x - y plane. The simulations have been performed by means of the Metropolis Monte Carlo algorithm in the isothermal-isobaric ensemble [18]. Periodic boundary conditions were applied to the simulation box along with the minimum-image criterion. In this ensemble the trial moves are the random changes of the positions and the orientations of the particles and the change of the simulation box size. The maximum displacement, rotation and box size change were adjusted during the simulations to get 30% acceptance ratio for all types of trials. The length of the particles (L) sets the scale in the system. Both compression and expansion runs have been done by starting from isotropic and completely ordered solid configurations, respectively. In most of the cases 10^6 – 10^7 MC cycles were enough for equilibration and additional 10^5 MC cycles were used to obtain the statistical averages. The comparison of the results of the expansion and compression routes indicates that there is no measurable hysteresis. The equation of state, order parameter, positional

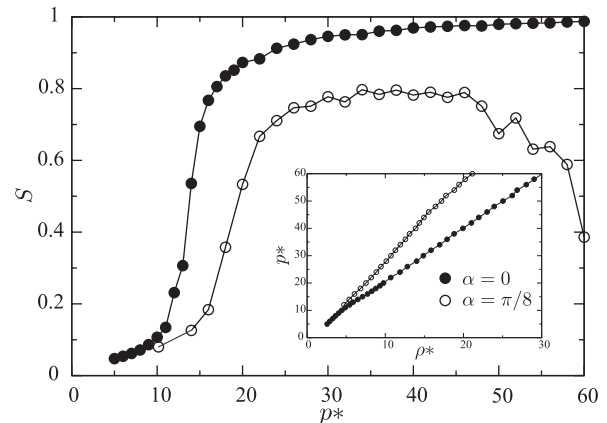


Fig. 2: Orientational order parameter of the banana-shaped hard needles for $\alpha = 0$ (filled circles) and $\alpha = \pi/8$ (open circles) and $N = 1000$. The inset shows the equation of state. The density and the pressure are dimensionless: $\rho^* = NL^2/A$ and $p^* = \beta p L^2$.

and orientational correlation functions were determined to characterize the structure of the equilibrium phases and the nature of the possible phase transitions. The nematic order parameter, S , and the orientational correlation function, $g_2(r)$, are defined as the largest eigenvalue of the traceless 2D symmetric tensor $T_{ij} = 2\langle\omega_i\omega_j\rangle - \delta_{ij}$ and $g_2(r) = \langle\cos(2\phi(0) - 2\phi(r))\rangle$. In these quantities $\langle\rangle$ denotes the ensemble average, ω_i is the i component of the particle's orientation given by $\omega = (\cos\phi, \sin\phi)$, δ_{ij} is the Kronecker delta function and r is the distance between two particles. For finite system size the nematic order parameter depends on the number of particles, N , and usually increases with the density. For straight needles the order parameter is zero in the thermodynamic limit ($N \rightarrow \infty$), instead of the true long-range order an algebraically decaying order occurs [11]. The orientational correlation function behaves as $g_2(r) \sim \exp(-\eta r)$ in the isotropic phase, while it becomes algebraic, $g_2(r) \sim r^{-\eta}$, in the high-density nematic phase. The transition between the two behaviours serves the critical density.

The order parameter of the finite-size system of bent-core needles differs from that of straight needles as it shows abnormal behaviour by its decreasing tendency with increasing pressure (density) above a certain value (see fig. 2). Remarkable differences between the straight and banana-shaped needles can be also seen in the pressure curves. The behaviour of the orientational correlation function is unusual, too, it decays exponentially in the isotropic (low pressure) phase, then it becomes algebraic at intermediate pressures, and it is again exponentially decaying at high pressures (see fig. 3). Interestingly the high pressure phase ($p^* = 60$) looks like an isotropic phase with stronger short-range orientational correlation than the nematic phase at $p^* = 40$. These results suggest that isotropic-nematic-isotropic re-entrance behaviour takes place with increasing pressure (density). However,

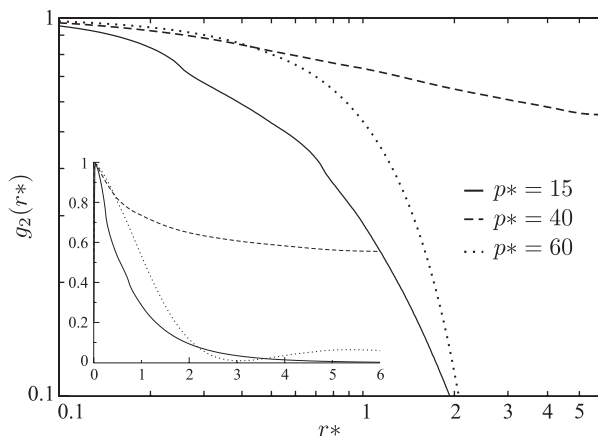


Fig. 3: Orientational correlation function of the banana-shaped hard needles for $\alpha = \pi/8$ and $N = 2000$. The pressure dependence of the correlation function is shown both in log-log and linear-linear scales. The pressure and the inter-particle distance are dimensionless: $r^* = r/L$ and $p^* = \beta p L^2$.

the closer inspection of the simulation snapshots, which are depicted in fig. 4, reveals that the low- and the high-density exponentially decaying structures are very different. While the particles are weakly correlated in the low-density isotropic system (fig. 4(a)), *i.e.* there is no orientational order, the particles are very ordered and form polar domains at high densities (fig. 4(c)). In addition to these differences, the ordered system is accompanied by the bend deformation with clock-wise rotation of the particles' polar axes, which has not been observed experimentally. The bend deformation of the polar domains cannot be attributed to the artificial external forces caused by the periodic boundary condition, but it is due to the bent-core shape-induced torque field. This field acts on the particles to maximize the free room available for the particles, which is no doubt the driving force in the packing process. However, fig. 4(d) shows for a larger value of α that the packing of the particles can be even more efficient by the positional ordering into a layered structure. We can see that the particles are not tilted in the layers and the polarity of the neighboring layers alternates and there is no net polarization in the box, *i.e.* the new phase is an antiferroelectric smectic A. Note that the inlayer polarization is due to the high up-down excluded-volume cost taking place between particles with opposite orientations (polarities). This smectic phase has been observed in the monolayer of the banana-shaped P-18-PIMB molecules adsorbed on HOPG surface [13].

Accepting that there is an intermediate density range where g_2 shows really power law decaying—even if it is difficult to define a sharp border between the power law and exponential behaviours—these results suggest the following scenario. The system has an unconventional nematic phase which is polar and locally very ordered but its global net polarization is zero. An approximate phase diagram can be seen in fig. 5. We can see that

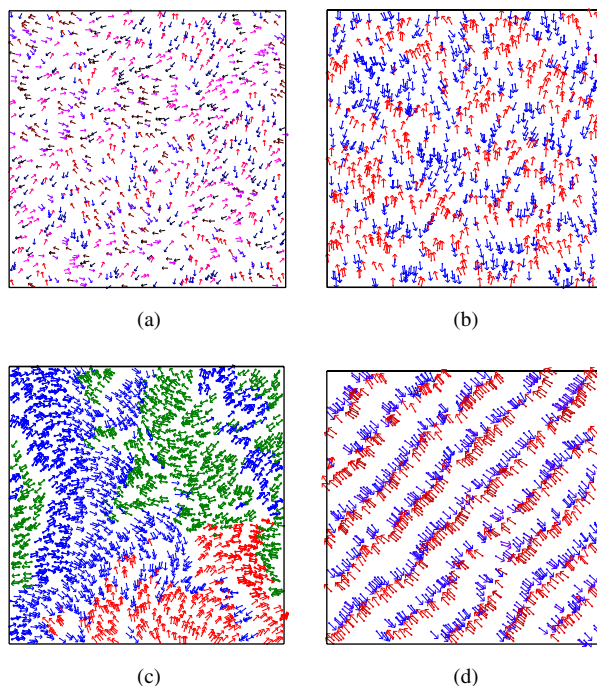


Fig. 4: (Colour on-line) Simulation snapshots of the detected mesophase structures: (a) isotropic ($p^* = 15$, $N = 1000$), (b) nematic ($p^* = 40$, $N = 1000$), (c) deformed nematic ($p^* = 60$, $N = 2000$) for $\alpha = \pi/8$ and (d) antiferroelectric smectic ($p^* = 55$, $N = 1000$) for $\alpha = 3\pi/8$. If the angle between two neighboring particles is less than $\pi/2$, both are shown with the same colour.

the increasing bend angle do not support the formation of the conventional nematic phase, but it gives rise to spontaneous bend deformation without net polarization. Moreover it stabilizes the antiferroelectric smectic phase to such an extent that the nematic order is completely missing for $\alpha \gtrsim \pi/5$. Note that the large bend angle of P-18-PIMB molecule can be the main reason why no nematic phase has been observed in the experiment of Gong and Wan [13].

We mention that the issue of the existence of algebraic decaying order is not completely resolved by our simulations because it may happen that the simulation box is not large enough and the correlation function is actually exponentially decaying in the bulk limit for all values of α . According to this scenario the system has no nematic phase at all, only a disordered isotropic phase and a smectic one. In the isotropic phase the short-range correlations become more stronger with the increasing density, but the excluded-volume interaction does not support the parallel alignment of the neighbouring particles. Therefore neither true nor quasi-long-range orientational order builds up. Based on our recent results we can not decide between the above two scenarios. However, we have no doubt that the locally ordered polar and spontaneously curved domains are stable. Another explanation—*e.g.* the system is becoming stuck in a glassy state—is out of

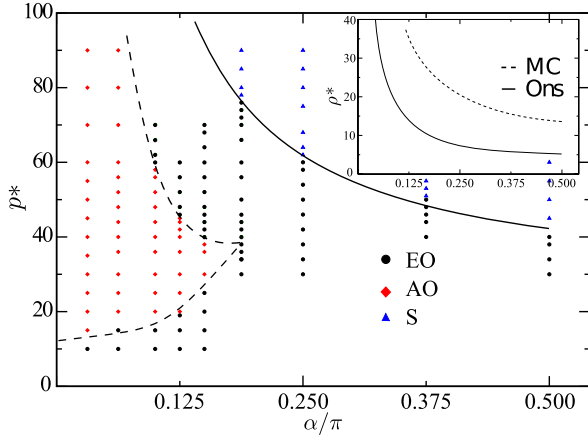


Fig. 5: (Colour on-line) Phase diagram of banana-shaped molecules in pressure-bend angle plane. The dashed curves are guide to the eyes to see the border of the mesophases (EO: exponentially decaying correlations, AO: algebraically decaying correlations, S: smectic). The symbols indicate the simulated pressure values. The inset shows the comparison of the Onsager theory and the MC simulation results for the lower border of the smectic phase in the density-bend angle plane, $\rho^* = NL^2/A$, $p^* = \beta pL^2$.

question because it would involve hysteresis in the equation of state, which is not observed in our simulation study.

Stability of the smectic phase. – Since the seminal work of Onsager [19], it is widely accepted that the second virial theory is capable to describe the bulk properties of mesophases. Onsager-type theories are quite successful in 2D, too [20]. It gives account of isotropic, nematic and smectic phases of various type of particle's shapes such as rectangle and zigzag etc. [21–23].

For the stability analysis of the smectic phase with respect to spatially uniform phase we search for the minimum of the free energy truncated at the second virial coefficient [19]. To maintain the simplicity of the theoretical treatment for the smectic phase, we do not include the effect of the orientational freedom, *i.e.* the Onsager theory of parallel particles is examined. Since the particle's shape does not have up-down symmetry we consider the extension of the theory for binary mixtures, where N_1 (up) and N_2 (down) particles are not allowed to rotate and they are antiparallel. The Onsager functional for this mixture is

$$\frac{\beta F}{A} = \sum_{i=1}^2 \rho_i \ln \rho_i - \rho_i + \frac{1}{d} \sum_{i=1}^2 \rho_i \int_0^d dy h_i(y) \ln(h_i(y)) + \frac{1}{2d} \sum_{i,j=1}^2 \rho_i \rho_j \int_0^d dy_1 h_i(y_1) \int_0^d dy_2 h_j(y_2) d_{\text{exc}}^{ij}(y_{12}),$$

where ρ_i is the number density of component i , d is the smectic period and h_i is the normalized distribution function in such a way that $\frac{1}{d} \int_0^d dy h_i(y) = 1$.

The input of the functional is the excluded distance between two particles of the components i and j , $d_{\text{exc}}^{ij}(y)$, which is related to the excluded area through $A_{\text{exc}}^{ij} = \int dy d_{\text{exc}}^{ij}(y)$. For the up-up and down-down pairs it is given by $d_{\text{exc}}^{11} = d_{\text{exc}}^{22} = 2|y| \tan(\frac{\alpha}{2}) H(\zeta - |y|) + (4a \sin \frac{\alpha}{2} - 2|y| \tan \frac{\alpha}{2})(H(2\zeta - |y|) - H(\zeta - |y|))$, while for the up-down configurations $d_{\text{exc}}^{12} = d_{\text{exc}}^{21} = (2a \sin \frac{\alpha}{2} - 2|y| \tan \frac{\alpha}{2}) H(\zeta - |y|)$, where $\zeta = a \cos(\frac{\alpha}{2})$. The stability of the spatially non-uniform smectic phase has been examined by the bifurcation analysis. Our numerical calculations show that out-of-phase pairs of smectic distribution functions, which are given by $h_1 = 1 + \epsilon \cos(qy)$ and $h_2 = 1 - \epsilon \cos(qy)$ for infinitesimally weak antiferroelectric smectic order, gives the lowest free energy, because the up and down species do not like to stay in the same layer. In addition to this result, writing the component densities as $\rho_1 = x\rho$ and $\rho_2 = (1-x)/\rho$, the fraction of up particles, x , is exactly 0.5 at the lowest free energy, *i.e.* the net polarization is zero in both phases. Substitution of the perturbed distribution functions h_1 and h_2 into the free energy, we get that the smectic free energy $\frac{\beta F}{A}|_S = \frac{\beta F}{A}|_N + C\epsilon^2$, where C depends on the wave number ($q = \frac{2\pi}{d}$). At the critical point C and $\frac{dC}{dq}$ must be zero. These two equations give the critical density (ρ_c) and the wave number (q_c) in the following simple forms:

$$\rho_c \approx \frac{5.3336}{\sin(\alpha)}, \quad q_c \approx \frac{4.9854}{\cos(\frac{\alpha}{2})}. \quad (1)$$

In agreement with the simulation results [11,12] no nematic-smectic phase transition occurs in the straight needle limit ($\alpha = 0$). Furthermore the increasing bend angle stabilizes the smectic order, which is always antiferroelectric. The inset of fig. 5 shows the simulation and theoretical critical curves together in the density-bend angle plane. We believe that the region of the smectic phase would shrink if the bifurcation analysis would be performed with respect to the more stable deformed or isotropic phases. However, the inclusion of the missing effects into the calculations would significantly over-complicate the calculations without resulting analytical equations for the phase boundary.

Theory of spontaneous bend. – Now we show that the spontaneously deformed locally ordered structure can exist in the system of bent-core needles using the second virial theory. It is well known that the free energy of the 2D hard disks truncated at the second virial coefficient (B2) can be written as

$$\frac{\beta F}{A} = \rho(\ln \rho - 1) + \rho^2 B_2, \quad (2)$$

where $\beta = 1/k_B T$, A is the surface area and ρ is the number density. B_2 is the half of the area surrounding a given disk, which is excluded to another disk, *i.e.* $B_2 = \frac{1}{2} A_{\text{exc}}$.

Onsager extended the second virial theory for anisotropic objects and showed that the entropy of mixing

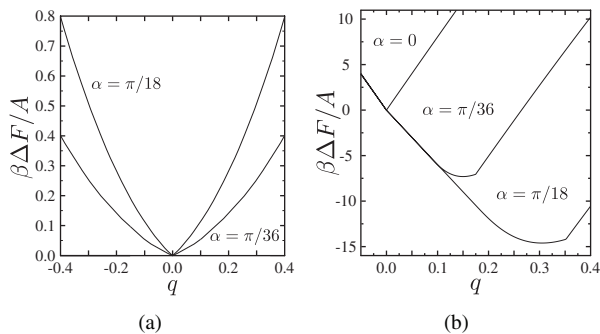


Fig. 6: The effect of splay and bend deformation in the free energy of parallel banana-shaped needles for increasing bend angle at the density $\rho^* = 22$: a) splay deformation, b) bend deformation. ΔF is the Free energy difference between the bended and spatially uniform structures, q is the deformation strength.

term due to the orientational freedom enters into the ideal part of the free energy and the orientational average of the excluded area gives the second virial term, *i.e.* $B_2 = \frac{1}{2}\langle A_{\text{exc}} \rangle$. To make the calculations for needles as simple as possible we assume that the particles are not allowed to rotate in a given position of the space. If all needles are parallel, the original second virial expression can be maintained by using the excluded area for parallel orientations, $A_{\text{exc}}^{\parallel}$. Such a situation corresponds to perfect and spatially uniform nematic order without any deformation. To include the spatially varying nematic director field into the calculations, we allow the particles to change their orientations according to the prescribed deformation. If the orientations of the particles are parallel to the spatially varying nematic director $\mathbf{n}(\mathbf{r})$, the free energy depends on the strength of the deformation q , *i.e.*

$$\frac{\beta F}{A} = \rho(\ln \rho - 1) + \frac{1}{2}\rho^2 A_{\text{exc}}(q), \quad (3)$$

where

$$A_{\text{exc}}(q) = \int d^2r H(\sigma(\boldsymbol{\omega}, \mathbf{n}(\mathbf{r}_0), \mathbf{n}(\mathbf{r})) - |\mathbf{r} - \mathbf{r}_0|). \quad (4)$$

Here H is the Heaviside step-function, σ is the distance of closest approach and $\boldsymbol{\omega} = \mathbf{r}/r$ is the centre-to-centre unit vector between two particles with orientations parallel with the nematic directors at the points \mathbf{r}_0 and \mathbf{r} according to the prescribed deformation. Assuming that $\mathbf{n}(\mathbf{r}_0) = (1, 0)$, the splay and bend deformations are given by $\mathbf{n}(\mathbf{r}) = (1, qy)$ and $\mathbf{n}(\mathbf{r}) = (1, -qx)$, respectively. Note that these expressions are only valid for weak deformations, which is justified on molecular length scale. Furthermore the free energy of parallel particles can be recovered for $q = 0$, because eq. (4) gives $A_{\text{exc}}(q = 0) = A_{\text{exc}}^{\parallel}$. Figure 6 shows the q dependence of the free energy for splay and bend deformations for bent-core needles. It can be seen that the uniform nematic phase resists against the splay deformation as the splay always increases the free energy for both positive and negative q . Moreover the

resistance becomes stronger with increasing bend angle. The situation is quite different for the bend deformation, because the free energy has the minimum for $q > 0$, *i.e.* the bend deformed nematic can be more stable than the spatially uniform one. We note that the bended structure is only locally polar and displays clockwise rotations which agrees with the positive value of q at equilibrium. The net polarization is zero due to the spatially varying (bended) nematic director field.

According to the Frank's elastic theory [24], the free energy of 2D nematics can be written as

$$F = F_0 + \frac{1}{2} \int d^2r (K_{\parallel}(\mathbf{n} \times \nabla \times \mathbf{n})^2 + K_{\perp}(\nabla \cdot \mathbf{n})^2), \quad (5)$$

where F_0 is the free energy of the undeformed nematic, \mathbf{n} is the nematic director K_{\parallel} and K_{\perp} are the elastic constants of bend and splay deformations. It is clear that any type of deformation increases the free energy of the undeformed nematic, *i.e.* eq. (5) is not able to explain the above results. To extend the Frank theory for bended nematics we need a term in eq. (5) which is linear in the deformation. For this reason we use \mathbf{m} unit vector, which is perpendicular to the nematic director, *i.e.* $\mathbf{m} = (n_y, -n_x)$. With this change we only permute the splay and bend deformation in eq. (5), because $\mathbf{n} \times \nabla \times \mathbf{n} = \mathbf{m} \nabla \cdot \mathbf{m}$. With the help of \mathbf{m} it is possible to construct a Frank free energy, which favours the bended nematic state. We do this by adding a linear torque term to the deformation free energy:

$$F = F_0 + \frac{1}{2} \int d^2r (K_{\parallel}(\nabla \cdot \mathbf{m})^2 - 2h \nabla \cdot \mathbf{m}), \quad (6)$$

where h is the bend torque-field parameter and the K_{\perp} term is omitted. Equation (6) was originally devised for polar nematic phase by Pleiner and Brand [25]. Note that the above equation is the analogue of the Frank free energy of cholesteric phase [26]. Inserting the bend director field ($\mathbf{n} = (1, -qx)$) into the above equation we get that $F/A = K_{\parallel}q^2/2 - hq$, which has the minimum at $q = h/K_{\parallel}$ in agreement with our results based on Onsager theory.

In the light of our results, the main issue is whether the bended nematic phase can exist or not in two dimensions. In this regard we believe that no definite answer can be drawn because of the shortcomings of the applied methods. The simulation suffers from the finite-size effects and the aligning effect of the periodic boundary condition, while the Onsager theory neglects the orientational fluctuations and the contributions of higher virial terms. No doubt, these effects have impact on the stability of algebraically decaying nematic order. The straight needles have an extra symmetry (rotation by π) compared to the bent-core particles which is the manifestation of the different symmetry properties of the interparticle interactions. We raise the issue that this symmetry breaking of the interaction may exclude the possibility of algebraic order. This idea is supported by our Frank's elastic analysis, which shows that a local torque field acts between the particles. This special field may totally suppress the

border between the low- and high-density structures, since the torque field always gives rise to a clockwise rotation in the structure of the fluid at any density. To answer for this fundamental issue, the possibility of 2D nematic order for particles interacting with non-separable potentials should be resolved first [27]. However, our results agree very well in one respect that a bended structure with clockwise rotation, which is locally polar and ordered, does exist in 2D systems of hard bent-core needles.

In summary it has been proved by the MC simulation and Onsager theory that the polar feature of the excluded-volume interaction alone stabilizes the locally nematic deformed structure and antiferroelectric smectic phase in two dimensions. Our results are in agreement with the experimental findings of Gong and Wan [13], that banana-shaped molecules can form antiferroelectric smectic structure in 2D. Our theory can be a good start for the examination of other polar-shaped molecular systems like the diblock polyisocyanides, which shows bilayer smectic order on HOPG substrate [28]. To get deeper insight into the complex phase behaviour of banana-shaped molecules it is necessary to go beyond the present Onsager theory and take the effects of orientational fluctuations and the finite thickness of the particles into account. The application of the phase-field-crystal theory can be a step ahead along this path [29].

We acknowledge the financial supports from PAPIIT (grant No. IN104111) and CONACYT (grant No. 49874-F). The authors are grateful to FENOMECA for supports related to this work. JAM-G is grateful for the scholarship from CONACYT.

REFERENCES

- [1] MADSEN L. A., DINGEMANS T. J., NAKATA M. and SAMULSKI E. T., *Phys. Rev. Lett.*, **92** (2004) 145505.
- [2] ACHARYA B. R., PRIMAK A. and KUMAR S., *Phys. Rev. Lett.*, **92** (2004) 145506.
- [3] BATES M. A. and LUCKHURST G. R., *Phys. Rev. E*, **72** (2005) 051702.
- [4] GRZYBOWSKI P. and LONGA L., *Phys. Rev. Lett.*, **107** (2011) 027802.
- [5] NIORI T., SEKINE T., WATANABE J., FURUKAWA T. and TAKEZOE H., *J. Mater. Chem.*, **6** (1996) 1231.
- [6] LINK D. R., NATALE G., SHAO R., MACLENNAN J. E., CLARK N. A., KÖRBLOVA E. and WALBA D. M., *Science*, **278** (1997) 1924.
- [7] JÁKLI A., KRÜERKE D., SAWADE H. and HEPPKE G., *Phys. Rev. Lett.*, **86** (2001) 5715.
- [8] KUMAR S., *Biaxial liquid crystal electro-optic devices* (US Patent No. 7,604,850) 2009.
- [9] MARTÍNEZ-RATÓN Y., VARGA S. and VELASCO E., *Phys. Chem. Chem. Phys.*, **13** (2011) 13247.
- [10] JÁKLI ANTAL and SAUPE A., *One- and Two-Dimensional Fluids: Properties of Smectic, Lamellar and Columnar Liquid Crystals* (Taylor and Francis) 2006.
- [11] FRENKEL D. and EPPENGA R., *Phys. Rev. A*, **31** (1985) 1776.
- [12] VINK R. L., *Eur. Phys. J. B*, **72** (2009) 225.
- [13] GONG J.-R. and WAN L.-J., *J. Phys. Chem. B*, **109** (2005) 18733.
- [14] SCHERES L., ACHTEN R., GIESBERS M., DE SMET L. C. P. M., ARAFAT A., SUDHÖLTER E. J. R., MARCELIS A. T. M. and ZUILHOF H., *Langmuir*, **25** (2009) 1529.
- [15] WANG J., QIU L., JÁKLI A., WEISSFLOG W. and MANN E. K., *Liq. Cryst.*, **37** (2010) 1229.
- [16] LIU L., KIM H.-J. and LEE M., *Soft Matter*, **7** (2011) 91.
- [17] BISI F., ROSSO R., VIRGA E. G. and DURAND G. E., *Phys. Rev. E*, **78** (2008) 011705.
- [18] FRENKEL D. and SMIT B., *Understanding Molecular Simulation: From Algorithms to Applications*, 2nd edition (Academic Press, San Diego) 2002.
- [19] ONSAGER L., *Ann. N.Y. Acad. Sci.*, **51** (1949).
- [20] CHRZANOWSKA A., *Acta Phys. Pol. B*, **36** (2005) 3163.
- [21] MARTÍNEZ-RATÓN Y., VELASCO E. and MEDEROS L., *Phys. Rev. E*, **72** (2005) 031703.
- [22] MARTÍNEZ-RATÓN Y., *Liq. Cryst.*, **38** (2011) 697.
- [23] VARGA S., GURIN P., ARMAS-PEREZ J. C. and QUINTANA-H J., *J. Chem. Phys.*, **131** (2009).
- [24] FRANK F. C., *Discuss. Faraday Soc.*, **25** (1958) 19.
- [25] PLEINER H. and BRAND H. R., *Europhys. Lett.*, **9** (1989) 243.
- [26] VARGA S. and JACKSON G., *Mol. Phys.*, **109** (2011) 1313.
- [27] STRALEY J. P., *Phys. Rev. A*, **4** (1971) 675.
- [28] BANNO M., WU Z.-Q., NAGAI K., SAKURAI S.-I., OKOSHI K. and YASHIMA E., *Macromolecules*, **43** (2010) 6553.
- [29] WITTKOWSKI R., LÖWEN H. and BRAND H. R., *Phys. Rev. E*, **83** (2011) 061706.